Avoiding temporal distortions in tilted pulses

Daniel Kreier and Peter Baum*

Max Planck Institute of Quantum Optics and Ludwig-Maximilians-Universität München, Am Coulombwall 1, 85748 Garching, Germany
**Corresponding author: peter.baum@lmu.de*

Received March 8, 2012; revised April 26, 2012; accepted April 26, 2012;
posted April 27, 2012 (Doc. ID 164415); published June 12, 2012

Tilted femtosecond laser pulses, having an intensity front with an angle to the propagation direction, can be generated by a dispersive element and a lens or mirror for imaging. Here we show that conventional geometries, for example with a grating at Littrow's condition, produce significant temporal distortions over the beam profile. The aberrations are the result of a mismatch between the grating's surface and the object plane of the imaging system. This changes the chirp of the pulses over the beam profile and lengthens the pulses to picoseconds for millimeter-sized beams. The distortions can be avoided by choosing a geometry in which the propagation direction of the tilted pulses is perpendicular to the grating's surface.

OCIS codes: 320.0320, 050.2770, 230.7020.

Tilted femtosecond pulses propagate with an intensity front that has an angle with respect to the direction of propagation. Incidence on a surface can produce a lateral sweep of the intensity that is slower than the speed of light. This is useful for providing group and phase matching in otherwise inaccessible geometries. Examples are the research fields of ultrafast electron diffraction [1,2], x-ray lasers with traveling-wave excitation [3,4], parametric amplification [5], or terahertz pulse generation [6–9].

Pulse front tilt is linked to angular dispersion [10–12]. A simple method for generating tilted pulses consists of a dispersive element (for example, grating) and an imaging system, which compensates for the undesired spatial separation of the different frequencies. The imaging system reproduces the tilted pulses at a location in free space. There, all frequencies overlap at the same point, but come from different directions. For pulses at a central wavelength λ_0, the tilt angle γ is [12]

$$\gamma \approx \arctan\left(M\frac{\partial\theta_{\mathrm{out}}}{\partial\lambda}\bigg|_{\lambda_0}\lambda_0\right), \tag{1}$$

where $\theta_{\mathrm{out}}(\lambda)$ is the angle of the grating's diffracted beam and M is the demagnification factor of the imaging system. For example, a grating with 2000 lines per mm used at Littrow's condition ($\theta_{\mathrm{in}} = \theta_{\mathrm{out}} \approx 53°$) produces tilted pulses with $\gamma \approx 70°$ after an 1:1 imaging system. Perpendicular incidence on a surface produces an effective group velocity of ~0.37 c.

Most applications of tilted pulses require large beam diameters. In ultrafast diffraction, for example, the size of the beam determines the amount of surface to be excited. For terahertz generation, the pulse energy and beam diameter must be adjusted to achieve an optimized intensity for optical rectification. For x-ray lasers, the spot must be large for achieving efficient amplification of spontaneous emission. In addition, in all examples the pulses should have shortest duration and therefore require a large bandwidth. In these two regimes, femtosecond pulses and large beams, two effects become significant. First, Eq. (1) relates tilt angle and dispersion. One could therefore suspect that higher-order terms of the grating's dispersion may produce a nonlinear tilt, that is, "banana"-shaped pulses. Second, the grating induces temporal chirp [11]. The pulses become longer the farther they travel away from the grating; this is the mechanism of a grating compressor. The imaging system should reverse this chirp, but ray-tracing calculations predict a varying pulse duration at the target [13,14]. Both effects can severely limit the applicability of tilted pulses.

In this Letter, we report an experimental study of nonlinearity and temporal distortions in tilted femtosecond pulses. Our measurement is based on recording a cross-correlation between a tilted and a non-tilted pulse. Figure 1 shows the setup. The laser source is a long-cavity Ti:sapphire oscillator (Femtosource XL, Femtolasers GmbH), providing ~60 fs pulses at a central wavelength of $\lambda \approx 800$ nm with a repetition rate of 5.1 MHz and a pulse energy of ~450 nJ. The collimated beam is separated into two parts by a 50% beam splitter (BS). One beam is guided through a cylindrical lens ($f = 300$ mm) onto a grating; a linear focus with dimensions of $\sim 0.1 \times 5$ mm is achieved on the grating's surface (yz-plane). The first-order reflection comes off closely to Littrow's condition; that is, mostly back toward the incoming beam. Going slightly upward (y-direction),

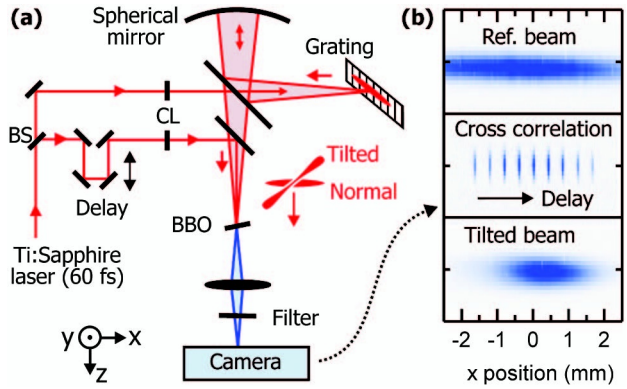

Fig. 1. Arrangement for measuring the shape of tilted femtosecond pulses at 800 nm. (a) Experimental setup of a cross-correlation between a tilted and a non-tilted pulse, where BS is a 50% beam splitter, CL represents cylindrical lenses, and BBO is a nonlinear crystal. (b) Pictures at 400 nm at the camera. Three contributions are produced: second harmonic of the reference beam (upper), second harmonic of the tilted beam (lower), and the cross-correlation signal for different delays (middle).

the beam is steered onto a large spherical mirror ($f_{\mathrm{mirror}} = 150$ mm), which provides a 1:1 imaging of the field at the grating onto a β-barium-borate crystal (BBO) with a thickness of 100 μm. There, the beam has a size of $\sim 3 \times 0.1$ mm (xy-plane). The other 50% of the laser is used as a non-tilted reference. It is widened by a telescope, mechanically delayed and also cylindrically focused onto the BBO crystal, with a slightly larger size of $\sim 5 \times 0.1$ mm (xy-plane). The angle between the two beams is $<4°$ and therefore negligible. With proper spatiotemporal overlap, sum-frequency generation provides a cross-correlation of the two incoming intensities.

The purpose of the cylindrical focuses is to increase the intensity for nonlinear interaction. There are three contributions to the output at ~400 nm: second harmonic of the tilted pulses coming from slightly above, second harmonic of the non-tilted pulses coming from slightly below, and a sum-frequency signal between the two. The output of the BBO crystal is imaged onto a camera (USBeamPro, Photon, Inc.). We applied a lens ($f =$ 60 mm) or a spherical mirror ($f = 200$ mm) with similar results. A spectral filter was used to suppress components around 800 nm and a slit was used to reject the two static contributions.

The cross-correlation signals are narrow strips, because sum frequency is only generated where the tilted and non-tilted pulses overlap in time; see depicted pulses in Fig. 1(a). Scanning the delay produces a sweep from left to right, which indicates the tilt. For each delay, we evaluated two parameters of the cross-correlation strips: central position and width. The positions provide a picture of the delay versus position, that is, the tilt. The widths provide the effective durations of the tilted pulse at all positions over the beam profile.

We used this arrangement to study two geometries for the diffraction grating. First, we applied Littrow's condition (input and output beams close to parallel), as shown in Fig. 2(a). This represents the geometry reported in the literature. We used a grating with 2000 lines/mm and an incidence angle of 49°. The first-order beam exists at ~58° and imaging with a magnification of ~1 provides an angular dispersion of ~3.7 mrad/nm, corresponding to an expected pulse front tilt of ~71.5°.

Figure 2(b) shows the results. The upper panel shows the delay versus position. We observed a straight line with a tilt of ~71.9°. No evidence for deviations from a purely linear tilt was found, although our 60 fs pulses have a considerable bandwidth (~30 nm). Higher orders of the grating's dispersion did not produce a curved shape of the pulses.

The linearity of the tilt over the entire beam profile can be understood by assuming causality at the grating's surface. Incidence of the incoming pulse "excites" the grating only during femtosecond times. The imaging system (the spherical mirror) reproduces this time-dependent intensity at the image location (the BBO crystal). Hence, the intensity profile at the BBO resembles a spatiotemporal image of the grating's surface. In this description, the tilt is linear because the grating is flat (not curved). Nonlinearities in the dispersion are not causing curved pulses, as shown here experimentally.

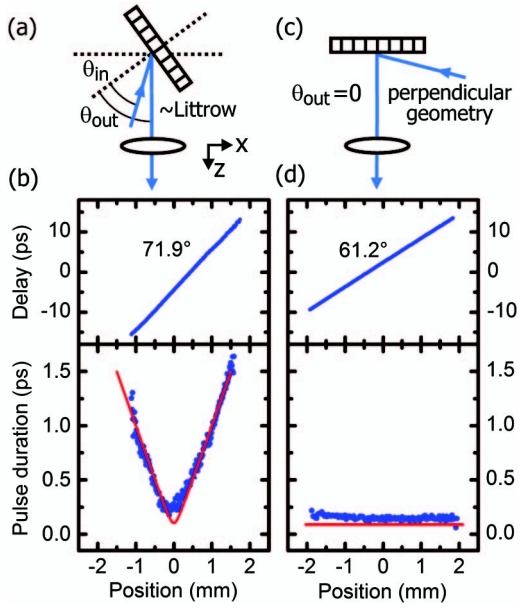

Fig. 2. Temporal distortions in tilted pulses for two different geometries of the grating. (a) Conventional arrangement with a Littrow grating. (b) Resulting pulse front tilt (upper panel, blue) and pulse duration (lower panel, blue) in dependence of the position within the beam. The red line is a calculation (see text). (c) Geometry to avoid aberrations, based on a perpendicular exit of the diffracted beam. (d) Resulting pulse front tilt (upper panel, blue) and pulse duration (lower panel, blue). The red line is a calculation.

Measuring the pulse duration over the beam profile produced a less favorable result. The blue dots in the lower panel of Fig. 2(b) show what we measured with near-Littrow geometry. A strong lengthening is evident at the edges of the beam; the width of the cross correlation is ~1 ps at a position 1 mm away from the beam's center. This is too much to be acceptable in femtosecond experiments.

The mechanism is based on temporal distortions. Besides dispersing the pulses spatially, the grating also produces a temporal chirp; this lengthens the pulses the more they travel away from the grating [11]. The spherical mirror reverses the angular and the temporal dispersion. At the image (the BBO crystal), the pulses should therefore be short again. It is indeed the case at the beam center, where the distances D_{gr} (between grating and spherical mirror) and D_{BBO} (between spherical mirror and BBO) provide an imaging condition ($1/f_{\mathrm{mirror}} = 1/D_{\mathrm{gr}} + 1/D_{\mathrm{BBO}}$). However, the grating is tilted with respect to the direction of the first-order beam. The imaging system's object plane (horizontal dotted line) has an angle θ_{out} with respect to the grating. Imaging is, therefore, imperfect for outer parts of the beam. The spherical mirror (or lens) is not fully reversing the temporal dispersion, and the pulses become chirped.

In order to calculate this, we invoke the geometry depicted in Fig. 2(a). At a lateral distance Δx from center, the distance D_{gr} is increased/reduced by $\Delta z = \Delta x \cdot \tan(\theta_{\mathrm{out}})$. At a distance Δz from the grating, a pulse with a Fourier-limited duration τ_0 acquires a duration $\tau(\Delta z)$ that is given by [11]

$$\tau(\Delta z) \approx \tau_0 \sqrt{1 + \frac{(2\ln 2)^2 \Delta z^2 \psi^4 \lambda_0^6}{\pi^2 c^4 \tau_0^4}}. \quad (2)$$

This is Eq. (23) of [11], rewritten for an angular dispersion $\psi = M \cdot (\partial\theta_{\mathrm{out}}/\partial\lambda)|_{\lambda_0}$ in wavelength units (rad/nm), and for pulse durations defined by full width at half maximum. Contributions originating from the spatial separation of the frequencies are neglected, because our beams are large in the plane of diffraction.

We also account for the apparatus function of our cross-correlation setup. Our camera has a pixel size of 6.7 μm, corresponding to a temporal resolution of $\tau_{\mathrm{camera}} \approx 6.7\ \mu\mathrm{m} \cdot \tan(\gamma)/c \approx 70$ fs, as a result of the lateral sweeps of the cross-correlation signal over the camera. The duration of the non-tilted pulses is $\tau_0 \approx 60$ fs. Considering these effects, the measured cross-correlation width is $\tau_{\mathrm{cross}} \approx \sqrt{\tau(\Delta z)^2 + \tau_0^2 + \tau_{\mathrm{camera}}^2}$. Compared to $\tau(\Delta z)$, this makes a slight difference only at very short durations of $\tau(\Delta z)$.

The red line in the lower panel of Fig. 2(b) shows the results. A good agreement to the experimental data is evident. It shows that the discrepancy between the grating and the imaging plane is indeed the reason for the observed temporal distortions and "bone"-shaped pulses at the target.

From these results it is evident how to avoid such aberrations. Coincidence of the grating with the object plane of the spherical mirror is required; the diffracted beam must exit the grating in a perpendicular direction. This principle was identified earlier [15]; here we provide a measurement with femtosecond pulses. Figure 2(c) depicts the geometry. In the experiment, we used a grating with 1100 lines/mm, an incidence angle of 61.5°, and a demagnification of ~1∶2 ($D_{\mathrm{gr}} \approx 450$ nm and $D_{\mathrm{BBO}} \approx 225$ mm). The expected pulse front tilt is ~60° in such a configuration. The grating's blaze and efficiency were not optimized for these angles; this will be a challenge for the future. Figure 2(d) shows the results. The tilt is linear, as expected from our grating's flat surface. In contrast to conventional geometry, the pulse duration is short over all of the beam profile [Fig. 2(d), lower panel]. The prediction by Eq. (2) for $\theta_{\mathrm{out}} = 0$, convoluted with the experimental resolution, produces the red trace. Theory deviates only slightly from the measured data. This shows that temporal distortions in tilted pulses can be avoided by choosing a geometry where the grating lies on the imaging system's object plane.

To generalize, the grating's angle θ_{out} determines the plane where the pulses are compressed. The combination of θ_{out}, θ_{in}, and M determines the pulse front tilt. In an application, both planes can be set as required by the sample's position and orientation. The depth-of-field of the imaging system defines the amount of temporal distortions.

We note some consequences of these results. First, in the field of intense terahertz generation, large beams are required to balance intensity and pulse energy [16]. A contact grating was proposed to minimize distortions [13]. In view of our results, an appropriate tilt of the grating also might be as successful. Second, in the field of x-ray lasers, travelling waves can be delivered to large targets with femtosecond duration everywhere. This opens up the possibility to use few-cycle petawatt lasers [17] for producing coherent x-ray beams. Third, in the field of ultrafast electron diffraction, temporal resolution in grazing incidence is essentially unlimited by velocity problems. If using single electrons [18], compression in microwaves or ponderomotive gratings [19,20], ultrashort laser pulses at megahertz repetition rates [21], and suitable arrangements for tilt, the regime of few-femtosecond resolution is in range.

This work was supported by the Munich-Centre for Advanced Photonics, the Rudolf-Kaiser-Stiftung, and the European Research Council (ERC grant "4D imaging"). The authors thank Matthias Mader for experimental assistance at the initial stage of this research.

References

1. P. Baum and A. H. Zewail, Proc. Nat. Acad. Sci. USA **103**, 16105 (2006).
2. P. Baum, D.-S. Yang, and A. H. Zewail, Science **318**, 788 (2007).
3. H. Daido, Rep. Prog. Phys. **65**, 1513 (2002).
4. R. Tommasini and E. E. Fill, Opt. Lett. **26**, 689 (2001).
5. T. Kobayashi and A. Shirakawa, Appl. Phys. B **70**, S239 (2000).
6. A. G. Stepanov, J. Kuhl, I. Z. Kozma, E. Riedle, G. Almási, and J. Hebling, Opt. Express **13**, 5762 (2005).
7. J. Hebling, K.-L. Yeh, M. C. Hoffmann, B. Bartal, and K. A. Nelson, J. Opt. Soc. Am. B **25**, B6 (2008).
8. K. Tanaka, H. Hirori, and M. Nagai, IEEE Trans. Terahertz Sci. Technol. **1**, 301 (2011).
9. M. C. Hoffmann and J. A. Fülöp, J. Phys. D **44**, 083001 (2011).
10. Z. Bor and B. Rácz, Opt. Commun. **54**, 165 (1985).
11. O. E. Martinez, Opt. Commun. **59**, 229 (1986).
12. J. Hebling, Opt. Quantum Electron. **28**, 1759 (1996).
13. L. Pálfalvi, J. A. Fülöp, G. Almási, and J. Hebling, Appl. Phys. Lett. **92**, 171107 (2008).
14. J. A. Fülöp, L. Pálfalvi, G. Almási, and J. Hebling, Opt. Express **18**, 12311 (2010).
15. J.-C. Chanteloup, E. Salmon, C. Sauteret, A. Migus, P. Zeitoun, A. Klisnick, A. Carillon, S. Hubert, D. Ros, P. Nickles, and M. Kalachnikov, J. Opt. Soc. Am. B **17**, 151 (2000).
16. J. A. Fülöp1, L. Pálfalvi, S. Klingebiel, G. Almási, F. Krausz, S. Karsch, and J. Hebling, Opt. Lett. **37**, 557 (2012).
17. Z. Major, S. A. Trushin, I. Ahmad, M. Siebold, C. Wandt, S. Klingebiel, T.-J. Wang, J. A. Fülöp, A. Henig, S. Kruber, R. Weingartner, A. Popp, J. Osterhoff, R. Hörlein, J. Hein, V. Pervak, A. Apolonski, F. Krausz, and S. Karsch, Rev. Laser Eng. **37**, 431 (2009).
18. M. Aidelsburger, F. O. Kirchner, F. Krausz, and P. Baum, Proc. Nat. Acad. Sci. USA **107**, 19714 (2010).
19. E. Fill, L. Veisz, A. Apolonski, and F. Krausz, New J. Phys. **8**, 272 (2006).
20. P. Baum and A. H. Zewail, Proc. Nat. Acad. Sci. USA **104**, 18409 (2007).
21. T. Ganz, V. Pervak, A. Apolonski, and P. Baum, Opt. Lett. **36**, 1107 (2011).